Hindawi Publishing Corporation
International Journal of Nuclear Energy
Volume 2014, Article ID 793934, 9 pages
http://dx.doi.org/10.1155/2014/793934

Research Article

Sensitivity Analysis of the TRIGA IPR-R1 Reactor Models Using the MCNP Code

C. A. M. Silva,[1] J. A. D. Salomé,[1] B. T. Guerra,[1] C. Pereira,[1] A. L. Costa,[1] M. A. F. Veloso,[1] M. A. B. C. Menezes,[2] and H. M. Dalle[2]

[1] *Departamento de Engenharia Nuclear, Escola de Engenharia, Universidade Federal de Minas Gerais, Campus Pampulha, Avenida Presidente Antônio Carlos 6627, 31270-901 Belo Horizonte, MG, Brazil*
[2] *Centro de Desenvolvimento da Tecnologia Nuclear, Comissão Nacional de Energia Nuclear, Campus Pampulha, Avenida Presidente Antônio Carlos 6627, P.O. Box 941, 31270-901, Belo Horizonte, MG, Brazil*

Correspondence should be addressed to C. Pereira; claubia@nuclear.ufmg.br

Received 11 April 2014; Accepted 23 July 2014; Published 9 September 2014

Academic Editor: Arkady Serikov

In the process of verification and validation of code modelling, the sensitivity analysis including systematic variations in code input variables must be used to help identifying the relevant parameters necessary for a determined type of analysis. The aim of this work is to identify how much the code results are affected by two different types of the TRIGA IPR-R1 reactor modelling processes performed using the MCNP (Monte Carlo N-Particle Transport) code. The sensitivity analyses included small differences of the core and the rods dimensions and different levels of model detailing. Four models were simulated and neutronic parameters such as effective multiplication factor (k_{eff}), reactivity (ρ), and thermal and total neutron flux in central thimble in some different conditions of the reactor operation were analysed. The simulated models presented good agreement between them, as well as in comparison with available experimental data. In this way, the sensitivity analyses demonstrated that simulations of the TRIGA IPR-R1 reactor can be performed using any one of the four investigated MCNP models to obtain the referenced neutronic parameters.

1. Introduction

The TRIGA IPR-R1 research reactor, located at the Centro de Desenvolvimento da Tecnologia Nuclear (CDTN) sponsored by Comissão Nacional de Energia Nuclear (CNEN) in Belo Horizonte, Brazil, operates since 1960 and it has been an important source of experimental data used in the processes of verification and qualification of several modelling processes of neutronic and thermal-hydraulic codes. Furthermore, the Laboratory for Neutron Activation Analysis of CDTN has been responsible for 70% of the analytical demand using the k_0 method of neutron activation analysis, established since 1995. Tests confirmed that the TRIGA IPR-RI reactor presented suitable characteristics to apply the method, mainly due to its stable and homogenous neutron fluxes. At that time, due to the symmetry of the core configuration and the rotary rack, no variations in neutron flux distribution in different channels were taken into account. The average thermal and epithermal fluxes were determined in the reactor rotating carousel facility (CF) [1, 2]. However, the reactor core configuration was changed in 2001 to enable a future power increase from 100 to 250 kW. This change consisted of four fuel rods added to the core, replacing the graphite dummy elements in the circular TRIGA core configuration [3]. In this configuration, the axial and radial neutron fluxes have not been measured and there are no experimental data about these parameters.

Previous studies evaluated the neutron flux in eleven irradiation channels of TRIGA comparing the estimated values by MCNP with experimental data [4–6]. The results presented good agreement when compared with experimental data.

Another previous work [7] investigated two modelling processes using MCNP code for the TRIGA IPR-R1 reactor. It presented some differences in the core elements dimensions according to technical documents used to perform such models. Moreover, one of them presented more geometrical detailing in relation to the other. Both models presented good

agreement with respect to the experimental data and they were verified in relation to the criticality calculation and reactivity changes.

During the modelling processes, there is not a fixed rule to perform it and then a large responsibility is passed to the code user in order to develop an adequate model scheme and each code user can model the same system, with the same code, in different ways. Therefore, sensitivity analysis including systematic variations in code input variables or modelling parameters must be used to help identify the relevant parameters necessary for a determined type of analysis, that is, to determine how "sensitive" a model is considering changes in the parameters values or structure model.

Now, to complete the process of sensitivity analysis, reactivity data to different control rod positions were obtained and compared with experimental available data. Furthermore, thermal and total neutron flux in the central thimble were calculated to be used and compared with experimental data in future works.

2. Methodology

2.1. TRIGA IPR-R1 Configurations. Detailed description of the TRIGA IPR-R1 reactor characteristics used to model such system in the MCNP5 code and the models developed can be found in [7]. The two models were identified as Model 1 and Model 2. The main difference between them is the degree of the geometry detailing, Model 2 being geometrically more detailed than Model 1. The main details added in Model 2 in relation to Model 1 are as follows.

(i) The active length of fuel element was discretized in 36 nodes.

(ii) The superior grid, inferior grid, and pneumatic tube were configured in this model.

(iii) Control rods guide tube is present.

(iv) The rotary rack groove is coated by aluminium layer.

(v) The samples of irradiation can be inserted in the rotary rack or in the central thimble or in the pneumatic tubes.

As described before, the differences between the models are in the geometry detailing. These models have the same materials composition obtained from [8] and they were configured according to the characteristics of TRIGA IPR-R1 [7]. In both models, the core was configured in the MCNP5 using a cylinder that contains water, fuel elements, radial reflectors, central tube, control rods, and neutron source. Each rod has a coordinate value. In these models, the rods were filled according to their individual characteristics. Around the core is the rotary rack with adequate groove to insert the samples to irradiation. The reactor was configured inside the pool where water surrounds the core and the rotary rack.

Beyond the detailing in the geometry for the two MCNP5 models analysed, there is a small divergence with respect to elements dimensions according to [8–10]. Therefore, the aim of this investigation is to identify how much the code results are affected by the different detailing and elements dimensions of the models analysing four different cases.

(i) Case 1—Model 1 and Dimension 1.

(ii) Case 2—Model 1 and Dimension 2.

(iii) Case 3—Model 2 and Dimension 1.

(iv) Case 4—Model 2 and Dimension 2.

In the simulations, Dimension 1 has the geometric values of previous studies [8, 9] and Dimension 2 presents the geometric values of the technical report [10]. Table 1 shows the core elements dimensions of the simulated models and information about criticality calculation simulations.

2.2. Evaluated Neutronic Parameters. To the sensitivity analyses, the neutronic parameters evaluated were the effective multiplication factor (k_{eff}), the reactivity (ρ), and the thermal and total neutron flux in central thimble as described in detail in the next subsections.

2.2.1. Effective Multiplication Factor (k_{eff}) and Reactivity. There are three control rods types in the reactor core: regulating rod, safety rod, and shim rod. Each control rod has a specific position according to its function [7]. The regulating rod provides fine reactivity control; the shim rod provides crude reactivity control; and the safety rod is used for reactor shutdown. Thus, the insertion of each control rod type generates different contributions to the core reactivity. In the simulations, each control rod type was individually inserted into the core where the k_{eff} was estimated for each 1.0 cm of control rod insertion. As the active length of control rods is 38 cm, there are 39 k_{eff} values to shim, safety, and regulating rod. In addition, the reactivity effects on total control rod insertion were compared with experimental data obtained from [11]. Therefore, the following core conditions were evaluated:

(a) all control rods withdrawn;

(b) individual and gradual insertion of shim rod;

(c) individual and gradual insertion of safety rod;

(d) individual and gradual insertion of regulating rod;

Experimental data with all control rods withdrawn can be obtained because TRIGA is the only nuclear reactor in this category that offers inherent safety. The safety of the reactor would be guaranteed even if the engineered features were bypassed and the control rods were rapidly removed. TRIGA is not ordinary light water reactor because much of its moderation of neutrons is due to the hydrogen that is mixed in with the fuel itself. Therefore, as the fuel temperature increases when the control rods are suddenly removed, the neutrons inside the hydrogen-containing fuel rod become faster than the neutrons outside in the cold water. These fast neutrons inside the fuel cause less fission and escape into the surrounding water. The end result is that the reactor automatically reduces the power in a few milliseconds [10, 11].

The MCNP5 estimates k_{eff} values. The k_{eff} variation (Δk_{eff}), reactivity (ρ), and control rods reactivity worth ($\Delta\rho$) were calculated using the following equations [7]:

$$\Delta k_{\text{eff}} = k_{\text{eff2}} - k_{\text{eff1}}; \quad (1)$$

$$\rho = \frac{k_{\text{eff}} - 1}{k_{\text{eff}}}; \quad (2)$$

$$\Delta\rho = \rho_2 - \rho_1 = \frac{1}{k_{\text{eff1}}} - \frac{1}{k_{\text{eff2}}}, \quad (3)$$

where the k_{eff1} and the k_{eff2} are the effective multiplication factors to all control rods withdrawn and inserted into the reactor core, respectively. As MCNP5 is a stochastic code, the standard deviation (σ_{ST}) estimated by this code is printed in the output file with the respective k_{eff} values. The relative error R was calculated using the following equation:

$$R = \frac{\sigma_{\text{ST}}}{k_{\text{eff}}}. \quad (4)$$

2.2.2. Neutron Flux into Central Thimble. Central thimble presents the maximum neutron flux due to its central position [8]. This tube is very important due to its application to sample irradiation. In the simulations, it was represented by a cylindrical cell where the neutron flux inside this cell was performed using the FMESH card of MCNP5 code. This feature allows the user to tally particles on a mesh independent of the problem geometry [12]. In the models, there are 56 cylindrical meshes with the same diameter of central thimble inside the cylindrical cell to estimate the neutron flux inside each mesh. For neutron flux analysis in the central thimble, the following core conditions were studied:

(a) all control rods withdrawn;

(b) only the shim rod totally inserted into the core;

(c) only the safety rod totally inserted into the core;

(d) only the regulating rod totally inserted into the core.

The MCNP5 estimates the flux using the source specified by the user. This estimation does not match the actual neutron source of the reactor. Thus, it is necessary to normalize the flux values initially calculated by MCNP5. In the simulation, this normalization was performed using the following equation [12]:

$$\phi_N = \phi_{\text{MCNP}} \times \left(\frac{P \times \nu}{Q \times k_{\text{eff}}}\right), \quad (5)$$

where ϕ_N is the normalized flux; ϕ_{MCNP} is the flux estimated by MCNP5; P is the reactor power level; ν is the average number of fission neutrons; and Q is the recoverable energy per fission event. The values of ν, Q, and k_{eff} are calculated by MCNP5 and they can be obtained in the output file of the code. The user provides the power level (P). In this work, $P = 250$ kW.

3. Results

3.1. Reactivity Analysis. Table 2 presents the standard deviation (σ_{ST}) and relative error (R) to the k_{eff} calculated by MCNP5 code. In addition, it shows the computation time (CT) for each case. According to [12], the values are reliable when the relative error $R < 0.10$. Table 2 shows that the relative error is around 0.011% and, therefore, the calculated k_{eff} values are acceptable. In addition, Table 2 shows that Cases 3 and 4 (configured with Model 2) present CT bigger than those for Cases 1 and 2 (configured with Model 1). This behaviour is due to Model 2 presenting more detailed geometry than Model 1. The MCNP code spends more time to follow particles in detailed geometries due to the increase of the number of surfaces and volumes. The code tracks particles through the geometry; it calculates the intersection of a track's trajectory with each bounding surface and finds the minimum positive distance to an intersection. MCNP finds the correct cell that the particle will enter by checking the sense of the intersection point for each surface listed for the cell. When a complete match is found, MCNP has found the correct cell on the other side and the transport continues [12]. Therefore, a large number of surfaces will spend more computational time.

Table 3 presents the values of k_{eff}, ρ, Δk_{eff}, and $\Delta\rho$ when the shim, safety, or regulating rod is totally inserted into core. This table shows these parameters to four studied cases and to experimental data (ED). The k_{eff1} represents the effective multiplication factor to all control rods withdrawn and k_{eff2} is the effective multiplication factor due to only one of the control rods (shim, safety, or regulating) inserted into the core.

The investigated cases have the same behaviour when the shim, the safety, or the regulating rod is inserted in the reactor core (see Table 3). In these cases, the insertion of shim rod induces the highest Δk_{eff}, while the insertion of regulating rod causes the smallest Δk_{eff}. In this way, the shim rod presents the highest $\Delta\rho$ while the regulating rod presents the lower value of $\Delta\rho$. On the other hand, for the safety and shim rods the Δk_{eff} and $\Delta\rho$ values are similar. The difference between the behaviours of such rods is due to their positions in the core. The regulating rod is located in the periphery of the core while the safety and shim rods are positioned near to the core centre. The simulated cases present the same behaviour of the experimental data.

Table 4 presents the difference between the calculated values (Cases 1, 2, 3, and 4) and the experimental data (ED). Such difference was calculated as

$$\text{Difference} = (\text{Calculated Value} - \text{Measured Value}). \quad (6)$$

Comparing Cases 1 and 2 (Model 1) or Cases 3 and 4 (Model 2), Cases 1 and 3 (Dimension 1) present the lowest value of the analysed difference. In comparison with the experimental data, Dimension 1 presents values of k_{eff} and ρ slightly overestimated while Dimension 2 presents values slightly underestimated.

As shown in Table 1, the fuel radius of aluminium element for Dimension 2 is smaller than for Dimension 1. Moreover, the central zirconium radius of stainless steel element in Dimension 2 is higher than in Dimension 1. These differences

Table 1: Main data of simulated models.

Modified elements description		Dimension 1 (cm)	Dimension 2 (cm)
Active core	Outer radius	22.098	22.060
Annular reflector	Inner radius	22.730	23.050
	Outer radius	53.140	53.500
	Height	53.950	56.000
Annular reflector cladding	Inner radius	22.098	22.060
	Outer radius	54.410	54.500
	Height	55.855	58.000
Rotary rack groove	Inner radius	29.883	29.050
	Outer radius	36.957	38.509
Graphite element	Graphite radius	1.799	1.789
Aluminium fuel element	Fuel radius	1.790	1.780
	Cladding inner radius	1.799	1.789
Stainless steel fuel element	Central zirconium radius	0.286	0.318
	Cladding outer radius	1.865	1.880
Control rods	Cladding inner radius	1.060	0.965
	Cladding outer radius	1.111	1.110

Information of criticality calculation	Dimensions 1 and 2
kcode particles number	100,000
Simulated cycles number (skipped)	515 (15)
Fission source	Punctual source at origin of system
Machine processor	System: OpenSUSE 12.1 Total memory (RAM): 94.5 GB Processor Intel (R) Xeon (R) CPU X5690 @ 3.47 GHZ Speed: 1,596 MHz Core number: 24

Table 2: Estimated parameters by MCNP5 code in the simulations.

Case type	Evaluated parameter	Control rod totally inserted			
		Shim	Safety	Regulating	No rods
Case 1	k_{eff}	0.99603	0.99741	1.01809	1.02236
	σ_{ST}	0.00011	0.00011	0.00011	0.00011
	R (%)	0.01104	0.01103	0.01080	0.01076
	CT (min)	36.14	35.55	35.73	36.20
Case 2	k_{eff}	0.98772	0.98914	1.01016	1.01411
	σ_{ST}	0.00011	0.00011	0.00012	0.00012
	R (%)	0.01114	0.01112	0.01188	0.01183
	CT (min)	35.07	35.52	35.78	35.81
Case 3	k_{eff}	0.99644	0.99805	1.01851	1.02300
	σ_{ST}	0.00010	0.00011	0.00011	0.00011
	R (%)	0.01004	0.01102	0.01080	0.01075
	CT (min)	89.84	87.56	88.03	89.06
Case 4	k_{eff}	0.98479	0.98627	1.00702	1.01126
	σ_{ST}	0.00011	0.00011	0.00011	0.00011
	R (%)	0.01117	0.01115	0.01092	0.01088
	CT (min)	86.94	88.38	88.57	88.43

Table 3: Results of the evaluated parameters to each simulated model.

Case type	Control rod totally inserted	Evaluated parameter					
		k_{eff1}	k_{eff2}	Δk_{eff} ($\times 10^{-2}$)	ρ_1 (pcm) ($\times 10^3$)	ρ_2 (pcm) ($\times 10^3$)	$\Delta\rho$ (pcm) ($\times 10^3$)
Case 1	Shim	1.02236	0.99603	−2.63300	2.18710	−0.39858	−2.58568
	Safety		0.99741	−2.49500		−0.25967	−2.44677
	Regulating		1.01809	−0.42700		1.77686	−0.41024
	No rods		1.02236	0.00000		2.18710	0.00000
Case 2	Shim	1.01411	0.98772	−2.63900	1.39137	−1.24327	−2.63464
	Safety		0.98914	−2.49700		−1.09792	−2.48929
	Regulating		1.01016	−0.39500		1.00578	−0.38559
	No rods		1.01411	0.00000		1.39137	0.00000
Case 3	Shim	1.02300	0.99644	−2.65600	2.24829	−0.35727	−2.60556
	Safety		0.99805	−2.49500		−0.19538	−2.44367
	Regulating		1.01851	−0.44900		1.81736	−0.43093
	No rods		1.02300	0.00000		2.24829	0.00000
Case 4	Shim	1.01126	0.98479	−2.64700	1.11346	−1.54449	−2.65795
	Safety		0.98627	−2.49900		−1.39211	−2.50558
	Regulating		1.00702	−0.42400		0.69711	−0.41636
	No rods		1.01126	0.00000		1.11346	0.00000
Experimental Data [8, 9]	Shim	1.01859	0.99418	−2.44100	1.82507	−0.58541	−2.41048
	Safety		0.99615	−2.24400		−0.38649	−2.21156
	Regulating		1.01434	−0.42500		1.41373	−0.41134
	No rods		1.01859	0.00000		1.82507	0.00000

Table 4: Difference between the calculation and experimental data (ED).

Inserted control rod	Case 1		ED		Difference	
	k_{eff}	ρ	k_{eff}	ρ	k_{eff}	ρ
Shim	0.99603	−0.00399	0.99418	−0.00585	0.00185	0.00186
Safety	0.99741	−0.00260	0.99615	−0.00386	0.00126	0.00126
Regulating	1.01809	0.01777	1.01434	0.01414	0.00375	0.00363
No rods	1.02236	0.02187	1.01859	0.01825	0.00377	0.00362
Inserted control rod	Case 2		ED		Difference	
	k_{eff}	ρ	k_{eff}	ρ	k_{eff}	ρ
Shim	0.98772	−0.01243	0.99418	−0.00585	−0.00646	−0.00658
Safety	0.98914	−0.01098	0.99615	−0.00386	−0.00701	−0.00712
Regulating	1.01016	0.01006	1.01434	0.01414	−0.00418	−0.00408
No rods	1.01411	0.01391	1.01859	0.01825	−0.00448	−0.00434
Inserted control rod	Case 3		ED		Difference	
	k_{eff}	ρ	k_{eff}	ρ	k_{eff}	ρ
Shim	0.99644	−0.00357	0.99418	−0.00585	0.00226	0.00228
Safety	0.99805	−0.00195	0.99615	−0.00386	0.00190	0.00191
Regulating	1.01851	0.01817	1.01434	0.01414	0.00417	0.00403
No rods	1.02300	0.02248	1.01859	0.01825	0.00441	0.00423
Inserted control rod	Case 4		ED		Difference	
	k_{eff}	ρ	k_{eff}	ρ	k_{eff}	ρ
Shim	0.98479	−0.01544	0.99418	−0.00585	−0.00939	−0.00959
Safety	0.98627	−0.01392	0.99615	−0.00386	−0.00988	−0.01006
Regulating	1.00702	0.00697	1.01434	0.01414	−0.00732	−0.00717
No rods	1.01126	0.01113	1.01859	0.01825	−0.00733	−0.00712

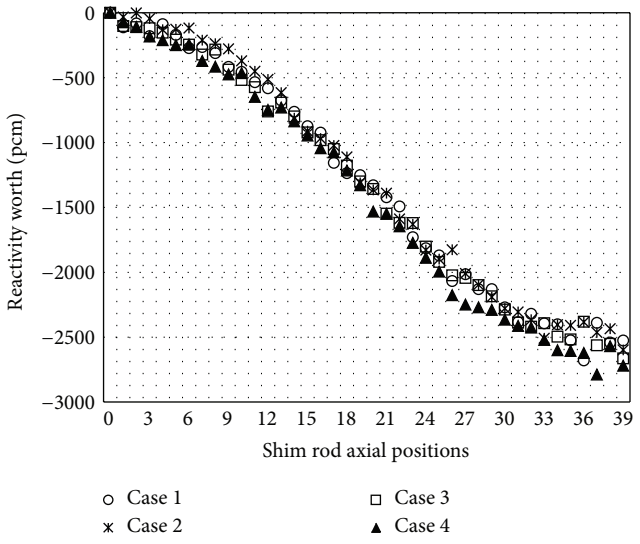

Figure 1: Reactivity worth ($\Delta\rho$) of gradual shim rod insertion.

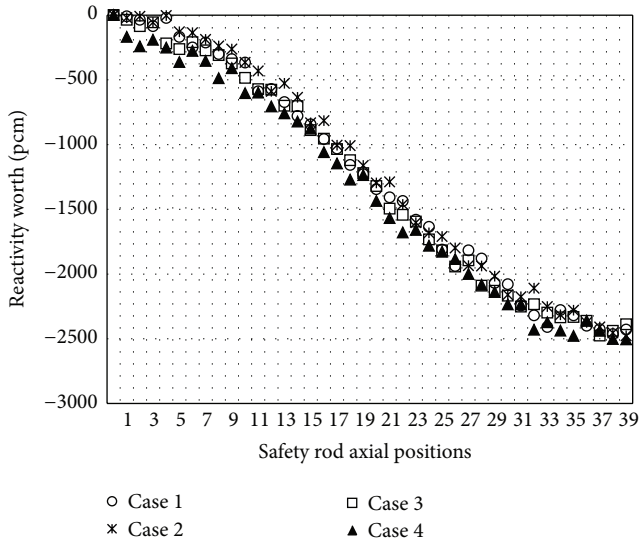

Figure 2: Reactivity worth ($\Delta\rho$) of gradual safety rod insertion.

cause small decreasing of fissile material in the reactor core reducing the values of k_{eff} and ρ parameters. Furthermore, Dimension 1 presents outer radius of active core higher than Dimension 2. Then, the active core in Cases 1 and 3 presents more water volume than in Cases 2 and 4. As the water is a moderator material, its largest volume in Cases 1 and 3 causes probably an increase in the thermal fission. Consequently, Cases 1 and 3 presented k_{eff} values increased in comparison with Cases 2 and 4.

Although Cases 1 and 3 as well as Cases 2 and 4 have the same dimensions, Cases 3 and 4 have more detailed geometry (Model 2) which presents grid plates and control rods guide tube. In Cases 1 and 2 (Model 1), the volume of these elements is filled with water. Therefore, Model 1 presents water volume bigger than Model 2. As the water is a moderator material, Cases 1 and 2 (Model 1) have k_{eff} value bigger than Cases 3 and 4 (Model 3) (see Table 4).

Figures from 1 up to 3 show the evolution of the $\Delta\rho$ for 39 axial positions of the shim, safety, and regulation control rods, respectively. In the figures, the zero position ("0") represents total withdraw and the thirty-nine position ("39") represents total insertion of control rods. As mentioned before, (3) was applied to calculate the control rods reactivity worth ($\Delta\rho$) to each of the 39 axial positions where the relative error of $\Delta\rho$ is around 4.9×10^{-4}. As it can be observed in the figures, the evolution of the $\Delta\rho$ presented the expected behaviour for all the simulated cases: as the control rods are inserted in the reactor core, the reactivity variations ($\Delta\rho$) increase. In agreement with the values presented in the Table 3, the shim and safety rods produce bigger reactivity worth (Figures 1 and 2) than the regulating rod (Figure 3) due to its radial core position. According to the Figures 1 and 2, the shim and safety rods provide around 2600 pcm each, while the regulating rod (Figure 3) provides about 500 pcm $\Delta\rho$ total.

3.2. Neutron Flux Analysis in the Central Thimble. Figures 4 and 5 present thermal and total neutron fluxes, respectively,

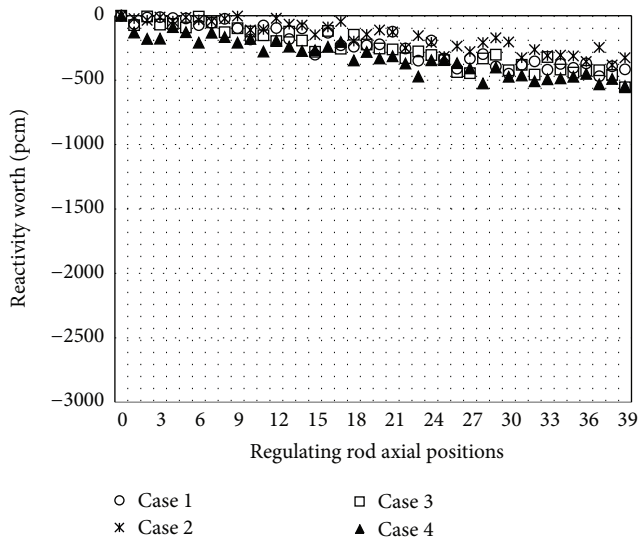

Figure 3: Reactivity worth ($\Delta\rho$) of gradual radual regulating rod insertion.

along the axial thimble positions for the four cases and for each case of control rod insertion. The ordinate axis represents the neutron flux values divided by 10^{12} and the abscissa axis represents the axial central thimble positions. As the central thimble was partitioned in 56 cylindrical cells in the model, the horizontal axis shows 56 positions from "–28" (bottom) up to "28" (top).

According to [12] the flux value is reliable when the relative error $R < 0.10$. In the simulated cases, the relative error of the estimated flux values is around 1%. Therefore, the calculated neutron flux values are statistically acceptable.

As it can be verified in Figures 4 and 5, the behaviour of the neutron flux distributions presents the typical "bell-shape." For the simulated cases, there are some small differences in the flux values where the biggest difference is 7.5%.

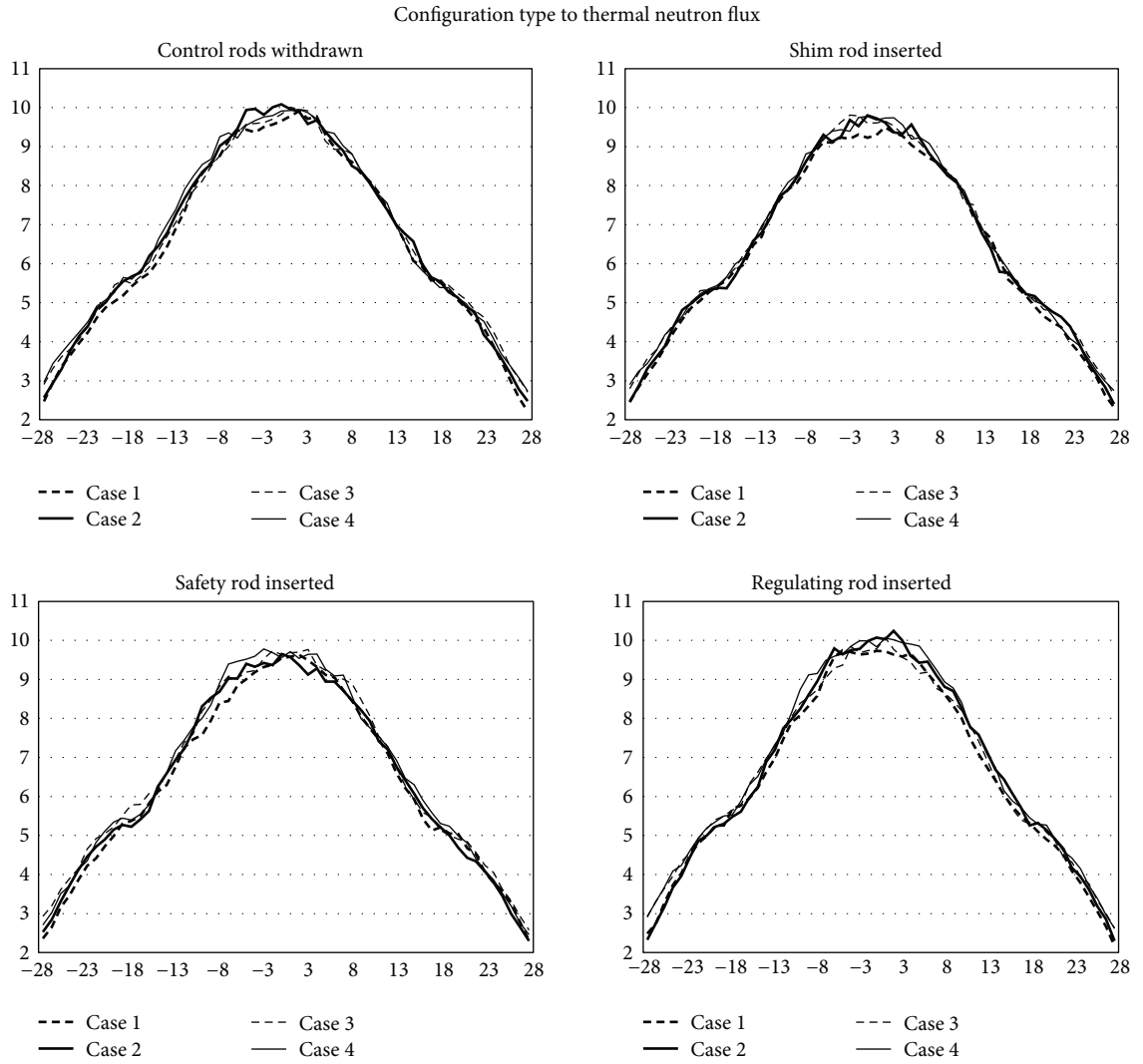

Figure 4: Thermal neutron flux ($\times 10^{12} \cdot cm^{-2} \cdot s^{-1}$) versus axial central thimble positions of the simulated models.

As it was analyzed previously, the shim and the safety rods moving cause the biggest $\Delta\rho$ (see Table 3). Consequently, the insertion of such rods will produce the higher flux reduction. This behaviour was verified in the simulated cases (see Figures 4 and 5); in spite of the effect of this control rods insertion, the flux depression is very small. In addition, Table 5 presents the average total flux value in the middle of central thimble where the smallest flux values are of shim and safety rods inserted.

Table 5: Average neutron flux in the middle of central thimble.

Inserted control rod	Thermal neutron flux ($\times 10^{12} \cdot cm^{-2} \cdot s^{-1}$)			
	Case 1	Case 2	Case 3	Case 4
Shim	9.2640	9.7634	9.6070	9.7285
Safety	9.5623	9.6109	9.6603	9.6336
Regulating	9.7181	10.0224	9.9171	9.9200
No rods	9.7271	10.0520	9.9273	9.9469
Inserted control rod	Total neutron flux ($\times 10^{12} \cdot cm^{-2} \cdot s^{-1}$)			
	Case 1	Case 2	Case 3	Case 4
Shim	19.3679	20.0651	20.1728	20.1664
Safety	19.8719	19.8786	20.0287	20.2220
Regulating	20.0979	20.5195	20.3159	20.7339
No rods	20.2836	20.7059	20.3656	20.9112

4. Conclusions

In this work, four cases of the TRIGA IPR-R1 reactor were analyzed using the MCNP5 code to estimate values of k_{eff}, ρ, Δk_{eff}, $\Delta\rho$ and neutron flux in central thimble in some different conditions of the reactor operation. The simulated Models 2 and 3 present corrections in the geometry dimensions of some core elements where Model 3 includes more geometry details than Model 2. The aim was to identify how much the code results could be affected according to these differences in the models.

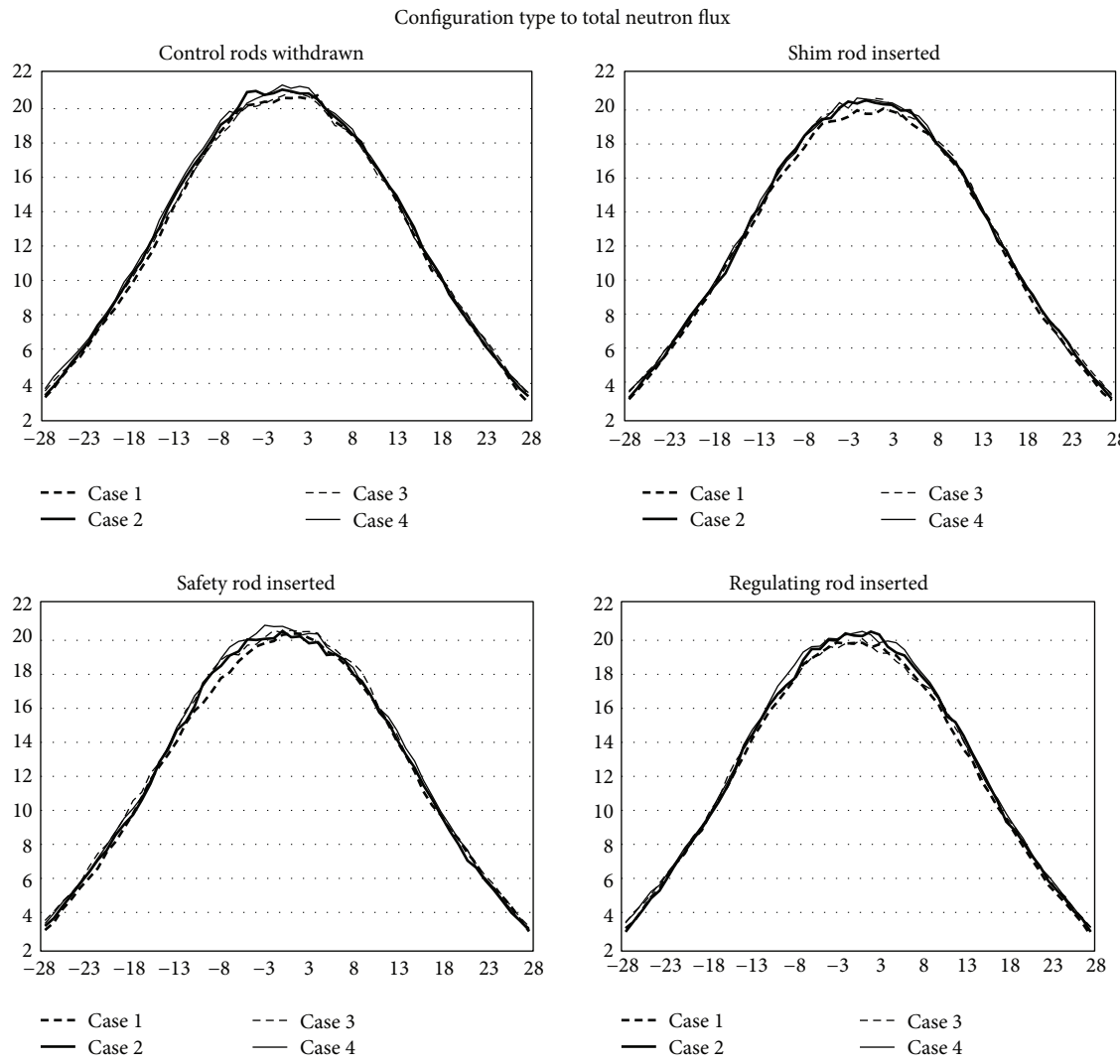

Figure 5: Total neutron flux ($\times 10^{12} \cdot cm^{-2} \cdot s^{-1}$) versus axial central thimble positions of the simulated models.

As the results demonstrated, the differences between the simulated models are small and therefore acceptable. In this way, the differences in the geometry dimensions detected in different reference works generated small variations in the evaluated neutronic parameters and the physical behaviour of these models is the same as all simulated models. The simulated models presented good agreement between them for the evaluated neutronic parameters and also when they considered experimental data. Therefore, the sensitivity analyses demonstrated that future works for the TRIGA IPR-R1 simulations can be performed using any of the four investigated models.

Conflict of Interests

The authors declare that there is no conflict of interests regarding the publication of this paper.

Acknowledgments

The authors are grateful to the Brazilian research funding agencies, CNEN (Brazil), CNPq (Brazil), CAPES (Brazil), and FAPEMIG (MG/Brazil), for the support.

References

[1] M. Â. B. C. Menezes and R. Jaćimović, "Optimised k0-instrumental neutron activation method using the TRIGA MARK I IPR-R1 reactor at CDTN/CNEN, Belo Horizonte, Brazil," *Nuclear Instruments and Methods in Physics Research A: Accelerators, Spectrometers, Detectors and Associated Equipment*, vol. 564, no. 2, pp. 707–715, 2006.

[2] M. A. B. C. Menezes and R. Jaćimović, "Validation of the k0_IAEA software using SMELS material at CDTN/CNEN, Brazil," *Journal of Radioanalytical and Nuclear Chemistry*, vol. 278, no. 3, pp. 607–611, 2008.

[3] H. M. Dalle and M. A. Veloso, "Monte Carlo simulation of TRIGA IPR-R1: reactivity worth, burnup, flux and power," in *Proceedings of the 3rd World TRIGA Users Conference*, Minas Gerais, Brazil, August 2006.

[4] J. A. D. Salomé, B. T. Guerra, C. Pereira et al., "Evaluation of the thermal neutron flux in samples of Al-Au alloy irradiated in the carrousel channels of the TRIGA MARK I IPR-R1 reactor using MCNP code," *Nuclear Engineering and Design*, vol. 41, pp. 576–583, 2014.

[5] J. A. D. Salomé et al., "Evaluation and modelling of the thermal neutron flux in samples in the caroussel channels of the TRIGA MARK I IPR-R1 reactor using Monte Carlo (MCNP)," in *Proceedings of the European Research Reactor Conference (PRFM '12)*, vol. 1, pp. 423–432, European Nuclear Society, Prague, Czech Republic, 2012.

[6] B. T. Guerra, C. A. M. Silva, C. Pereira et al., "Thermal neutron fluxes characterization in the irradiation channels of the IPR-R1 using monte carlo method," in *Proceedings of the Transactions of European Research Reactor Conference (RRFM '11)*, vol. 1, pp. 732–736, Bruxelas, European Nuclear Society, Rome, Italy, 2011.

[7] C. A. M. Da Silva, C. Pereira, B. T. Guerra et al., "MCNP5 modeling of the IPR-R1 TRIGA reactor for criticality calculation and reactivity determination," *Nuclear Engineering and Design*, vol. 241, no. 12, pp. 4989–4993, 2011.

[8] H. M. Dalle, *Simulação do Reator IPR-R1Utilizando Métodos de Transporte por Monte Carlo [Doctoral Thesis]*, Faculdade de Engenharia Química, Universidade Estadual de Campinas, Campinas, Brazil, 2005 (Portuguese).

[9] H. M. Dalle, C. Pereira, and R. G. P. Souza, "Neutronic calculation to the TRIGA Ipr-R1 reactor using the WIMSD4 and CITATION codes," *Annals of Nuclear Energy*, vol. 29, no. 8, pp. 901–912, 2002.

[10] M. A. Veloso, "Avaliação Termo-Hidráulica do Reator TRIGA IPR-R1 a 250 kW," Technical Document NI-EC3-05/05, CDTN/CNEN, Belo Horizonte, Brazil, 2005.

[11] R. M. G. P. Souza et al., "Resultados dos Testes Iniciais para o Aumento de Potência do Reator TRIGA IPR—R1, NI-IT4-01/01," Technical Document CDTN/CNEN, Belo Horizonte, 2001.

[12] T. E. Booth, F. B. Brown, J. S. Bull et al., "MCNP—a general monte carlo n-particle transport code (version 5)," Tech. Rep. LA-UR-03-1987, Los Alamos National Laboratory, 2003.